Monthly Notices
of the
ROYAL ASTRONOMICAL SOCIETY

MNRAS **495,** 3715–3721 (2020)
Advance Access publication 2020 May 23

doi:10.1093/mnras/staa1424

Origin of quasi-harmonic emission bands with fine structure in the dynamic spectra of high-frequency interpulses of the Crab pulsar

V. V. Zheleznyakov[1] and V. E. Shaposhnikov[1,2]★

[1] *Institute of Applied Physics of the Russian Academy of Sciences, Nizhny Novgorod, 603950, Russia*
[2] *National Research University High School of Economics, Nizhny Novgorod Branch, Nizhny Novgorod, 603005, Russia*

Accepted 2020 May 14. Received 2020 May 14; in original form 2020 February 19

ABSTRACT

We study the origin of quasi-harmonic emission bands with fine structure observed in the dynamic radiation spectra of high-frequency interpulses. The possible explanation of observed structure is based on the effect of double plasma resonance (DPR) at electron cyclotron harmonics realized in the magnetosphere of pulsar in a local radio emission source filled with non-relativistic plasma. The model of the source consists of neutral current sheet with a transverse magnetic field where plasma waves are generated due to DPR effect. It is shown that the emergence of emission bands and their frequency spacing are due to the inhomogeneity of the plasma and magnetic field along the current sheet, and their fine structure is due to the inhomogeneity of the current sheet in the direction orthogonal to it. Each quasi-harmonic emission band represents a system of elements of fine features of radiation that is generated by suprathermal electrons under DPR conditions. The observed upward drift of quasi-harmonic emission bands is due to the displacement of suprathermal electrons across the current sheet and an increase in the DPR frequencies with distance from the central plane of the layer.

Key words: radiation mechanisms: non-thermal – methods: analytical – pulsars: individual: NP0532.

1 INTRODUCTION

After the discovery of pulsars in 1967, consideration about the origin of their radio emission was mainly limited to a comparative analysis of the electromagnetic radiation mechanisms known in radio astronomy and plasma physics as applied to conditions in the vicinity of neutron stars. However, noticeable progress on this way was not achieved for two reasons: the uncertainty in these conditions (the parameters and structure of the magnetospheres) and the limited characteristics of the observed radio bursts (their 'simplicity'). And only after 40 yr did the situation change due to the discovery by Hankins and Eilek (Hankins & Eilek 2007; Eilek & Hankins 2016; Hankins, Eilek & Jones 2016). They first obtained the dynamic spectra of the microwave radiation of the Crab pulsar using a radio spectrograph with a high time and frequency resolution mounted on an antenna in Arecibo (Puerto Rico). One typical example of such spectra for phenomena in the composition of high-frequency interpulses (HFIPs) having a complex time-frequency structure is shown in Fig. 1.

It is seen in this figure that the dynamic spectrum of an individual pulse contains a system of quasi-harmonic emission bands (zebra pattern). With statistical averaging of the spectra of hundreds of bursts in a wide frequency range of 5–30 GHz, it was found by Hankins & Eilek (2007) and Hankins et al. (2016) that the emission band spacing $\Delta f_{\rm obs}$ increases linearly with the frequency $f_{\rm obs}$

$$\Delta f_{\rm obs} \approx 6 \times 10^{-2} f_{\rm obs}. \quad (1)$$

This ratio serves as the main argument in choosing the mechanism for generating these bursts. It indicates that the generation of different emission bands occurs in different parts of the source with a non-uniform magnetic field and plasma density. From Fig. 1, it is clear that each emission band has a fine structure: It consists of narrower (in frequency) elements that show a characteristic evolution in time. Each emission band begins with the appearance of a low-frequency element, which exists for a shorter time than the burst as a whole. Then there appears the next element, which is shifted towards the higher frequencies, etc. Each band contains 3–5 individual elements of the fine structure. Schematically, this evolution is more clearly shown in Fig. 2, where the bright elements in the four emission bands from Fig. 1 are represented as dark horizontal lines.

A careful examination of the dynamic spectrum in Fig. 1 and similar spectra published by Hankins and Eilek leads to the conclusion that the elements of the fine structure are not superimposed on the quasi-harmonic emission bands. They actually form these bands, and the observed frequency drift of the emission bands towards higher frequencies is due to the successive change of one bright

★ E-mail: sh130@ipfran.ru

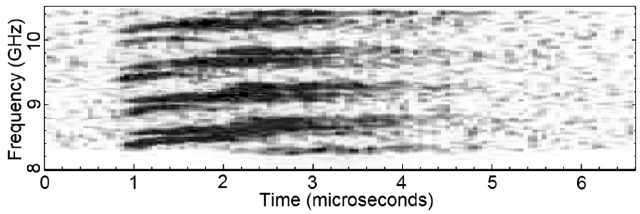

Figure 1. This is an example of dynamic spectra of high-frequency interpulse emission with a complex time-frequency structure. This figure is adapted from Eilek & Hankins (2006, fig. 4).

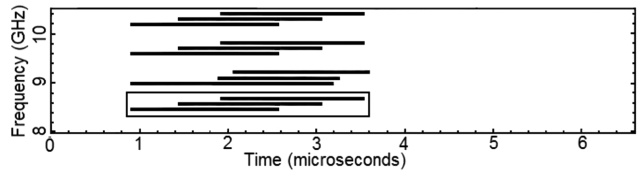

Figure 2. Schematic representation of the evolution of the dynamic spectrum (Fig. 1) with a fine structure of the emission bands. A fragment of the dynamic spectrum enclosed in a rectangle is analysed in Section 3 (see Fig. 7).

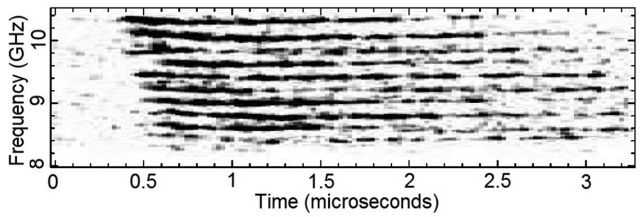

Figure 3. Rare type of the dynamic spectrum with the emission bands. This figure is adapted from Hankins et al. (2009, fig. 5).

element to another, higher frequency element at a later instance of time. This fact is also indicated by Hankins et al. (2016), who analysed a large number of pulses and concluded that the drift of the emission bands towards higher frequencies is due to the appearance of new elements in the band that are delayed in time and start at slightly higher frequencies.

Fig. 3 shows another, more rare type of the dynamic spectrum (Hankins, Rankin & Eilek 2009). In the observed frequency range 8–10 GHz, the dynamic spectrum exhibits a continuous fine structure of 10 elements, rather than individual emission elements grouped into quasi-harmonic bands. Note that an insufficiently high frequency resolution does not allow an unambiguous conclusion to be drawn whether a finer frequency structure similar to that observed in Fig. 1 exists inside the observed emission bands. We also note that the interval 8–10 GHz, in which radiation with the above-mentioned structure was observed, is too narrow to definitely judge the change in the emission band spacing. It is quite possible that it remains constant. The latter will be taken into account in Section 3 when explaining the dynamic spectrum depicted in Fig. 3.

Note that in both types of the dynamic spectrum, the signal lags as the radiation frequency is decreased. Hankins et al. (2016) relate this effect with the group delay of the signal directly in the local radiation source with a zebra pattern. It is discussed in detail in Zheleznyakov & Bespalov (2018).

Zheleznyakov, Zlotnik & Zaitsev (2012) pointed to the analogy of the structures of the dynamic spectrum in HFIP with a 'zebra' pattern in solar radio emission[1] and suggested that the emission mechanisms can be analogical, i.e. the HFIP emission mechanism is based on the effect of double plasma resonance (DPR) at electron cyclotron harmonics. In that paper, they also proposed a model of a local source in the form of a neutral current sheet with a transverse magnetic field moving with a subluminal speed around a neutron star. In an article by Zheleznyakov & Bespalov (2018), the conditions for the propagation of radiation in this source and its free exit beyond the source were studied.

Section 2 provides the necessary information from the DPR theory and the model of a local source in the form of a neutral current sheet with a transverse magnetic field. In Section 3, based on the DPR effect in the current sheet with transverse magnetic field, an explanation is given for the origin of quasi-harmonic emission bands with a fine structure. It is shown how, depending on the time evolution of the suprathermal electrons of the current sheet, two types of observed structures are realized in the dynamic spectra of HFIP.

2 PHENOMENON OF DPR AND A MODEL OF LOCAL SOURCE OF QUASI-HARMONIC BURSTS

The emission mechanism based on the DPR effect was first put forward for the interpretation of quasi-harmonic emission bands, the so-called 'zebra' pattern, in the dynamic spectra of solar radio emission (Kuijpers 1975; Zheleznyakov & Zlotnik 1975a, b, c). In plasma physics, DPR is the coincidence of the upper-hybrid resonance frequency f_{UH} with one of the harmonics of the electron cyclotron frequency sf_B

$$f_{UH} = \sqrt{f_B^2 + f_L^2} \approx s f_B. \tag{2}$$

Here, $f_L = \sqrt{e^2 N/\pi m}$ and $f_B = eB/2\pi mc$ are the Langmuir and cyclotron frequencies of electrons, respectively, s is the number of the cyclotron harmonics, N and B are the plasma density and the magnetic field in the generation region, respectively, e and m are the electron's charge and mass, respectively, and c is the speed of light. In a plasma with weak magnetic field, $f_L >> f_B$, as well as for high cyclotron harmonics $s \gg 1$, the DPR condition takes the form

$$f_L \approx s f_B. \tag{3}$$

The DPR effect is effective excitation due to the cyclotron instability (the increment increases by about one or two orders of magnitude) of electrostatic (plasma) waves propagating almost across the magnetic field. The increment increases in a narrow frequency range $\Delta f_r \ll f$ located above the cyclotron harmonic frequency $sf_B \approx f_{UH} \approx f$ (f is the frequency of the excited wave). Within our study, a slight difference of the frequency of the excited wave from the frequency of the cyclotron harmonic is not significant. For simplicity, we neglect this difference and assume that the wave excitation due to the DPR effect occurs at the cyclotron harmonic frequency, i.e. we assume that $f = sf_B = f_{UH}$. A detailed discussion of the emission mechanism of quasi-harmonic bursts based on the DPR effect can be found in Zheleznyakov (1996) and Zheleznyakov et al. (2016).

[1] It should be noted that in dynamic spectra with a zebra pattern in solar radio emission, the fine structure of emission bands similar to the fine structure of emission bands in HFIP is absent.

The main requirements to the source of the zebra pattern radiation generated due to the DPR effect in the pulsar magnetosphere were formulated from the analysis of observational data in Zheleznyakov et al. (2012) and Zheleznyakov & Bespalov (2018). It is assumed that the width of the pulse averaged profile is determined by a narrow radiation pattern formed during the subluminal motion of the source (Smith 1969; Zheleznyakov 1971). The stability of the rotation phase of the pulse averaged profile and its period, which coincides with the period of rotation of the neutron star, indicate that the source is located inside the light cylinder. A feature of the radiation pattern due to relativistic 'compression' is that the pulse width is independent of the radiation frequency (Zheleznyakov 1971, 1996)

$$\Delta t \approx \frac{P}{2\pi}\left(1-\beta^2\right)^{3/2}, \tag{4}$$

where P is the period of source rotation around the neutron star and $\beta = V_s/c$ (V_s is the linear velocity of the source). For the Crab nebula pulsar, $P \approx 3.3 \times 10^{-2}$ s. Independence of the width of the averaged pulse profile, which is characteristic of the HFIPs of the Crab pulsar (see e.g. fig. 1 in Eilek & Hankins 2016) is one of the arguments in favour of the relativistic model of the radiation pattern formation.

Relationship (4) makes it possible to determine the source rotation speed around the star: $\beta \approx 0.8$. This speed is achieved at a distance $R_s = V_s P/2\pi \approx 1.3 \times 10^8$ cm from the star (light cylinder radius $R_l \approx 1.6 \times 10^8$ cm). Subluminal motion of the source leads to the fact that the observed radiation frequency f_{obs}, which is connected with frequency f in the source by the Doppler relation

$$f_{obs} = f_{em}\frac{\sqrt{1-\beta^2}}{1-\beta\cos\theta} \tag{5}$$

for $\cos\theta \approx 1$ (θ is the angle between the radiation direction in the observer system and the source velocity), turns out to be about a factor of 3 higher than the corresponding frequency in the source ($f_{obs} \approx 3.2 f_{em}$).

According to the DPR condition given by equations (2) and (3), the cyclotron frequency f_B should be much less than the Langmuir frequency f_L. These conditions can be provided in a source with weak magnetic field and a relatively high electron density of the plasma, which is located in the magnetosphere of a pulsar having a strong magnetic field.

Fig. 4(a) shows a schematic representation of the emission region. Due to the curvature of the field lines, magnetic traps in the centre of the layer (shaded area) are formed, where suprathermal electrons with a non-equilibrium distribution function are concentrated. The DPR regions are indicated by a cross-hatching. Plasma waves are generated due to the presence of these suprathermal electrons in the layer. Fig. 4(b) shows a mathematical model of the magnetic field in the source formed by a current sheet and a transverse magnetic field superimposed on it (Zheleznyakov et al. 2012). This current sheet is a local formation sporadically appearing and disappearing in the pulsar magnetosphere [in this context, see Eilek & Hankins (2016)]. In Zheleznyakov & Bespalov (2018), the values of the plasma density $N \sim 10^{11}$ cm^{-3} and the magnitude of the transverse magnetic field $B_\perp \sim 10^2$ G at the centre of the sheet, which are necessary for the generation of zebra pattern radiation, were indicated. These values differ significantly from the values of the corresponding parameters in the magnetosphere surrounding the layer. The case is different at the periphery of the current sheet. High plasma density exists only in the centre of the current sheet and decreases at its periphery to the values in the surrounding magnetosphere. The

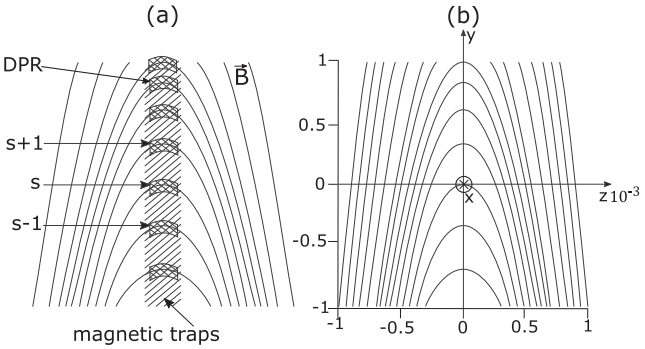

Figure 4. (a) Schematic representation of the source. The shaded band in the centre indicates a system of magnetic traps where suprathermal electrons with a non-equilibrium distribution function are concentrated. The DPR regions, where such electrons excite plasma waves due to the DPR effect, are indicated by a cross-hatching. (b) Model magnetic field created by a Harris current sheet with a transverse magnetic field superimposed on the layer. Cartesian coordinates y and z are normalized to the characteristic scales of changes in the layer parameters along the corresponding axes.

magnetic field increases towards the sheet periphery and reaches the values usually taken for the surrounding magnetosphere.

The plasma waves excited due to the DPR effect transform to electromagnetic waves with the frequency f_{em} as a result of two possible processes, namely Rayleigh scattering by plasma particles and induced Raman scattering (coalescence) of excited plasma waves by counter-running plasma waves with the formation of an electromagnetic wave escaping from the radiation source (Zheleznyakov et al. 2012). The first process occurs with the frequency preserved ($f_{em} = f_L$) and the second, with the frequency doubled ($f_{em} = 2f_L$). It should be noted that in the case of the Crab pulsar, the choice between these transformation processes is currently difficult and their relative effectiveness needs special analysis. Significant help with solving this problem could be provided by the dynamic spectra of individual bursts in a wide frequency range (at least with double frequency overlap). Unfortunately, the equipment used in the Hankins and Eilek observations for the simultaneous analysis of dynamic spectra was limited to a fairly narrow frequency range of about 2–4 GHz in the studied range from 5 to 30 GHz.

3 FORMATION OF SPECTRAL BANDS IN QUASI-HARMONIC BURSTS

We now discuss how the dynamic spectra of the Crab pulsar radiation with a zebra pattern, which are shown in Figs 1 and 3, can be formed on the basis of the DPR effect at electron cyclotron harmonics. We note first that in a homogeneous magnetoactive plasma ($f_L = const$ and $f_B = const$) it follows from the DPR condition (2) that a DPR can exist for only one value of the harmonic $s = \sqrt{1 + f_L^2/f_B^2}$. This leads to a high level of oscillation only at one frequency, $f = sf_B$. However, in a homogeneous plasma ($f_L \neq const$), both with a uniform magnetic field and in a more general case with a non-uniform magnetic field ($f_B \neq const$), the DPR effect takes place in the whole system of harmonics and is manifested in the dynamic spectra in the form of harmonic bands at $f_B = const$ or in the form of quasi-harmonic bands at $f_B \neq const$.

Following Zheleznyakov et al. (2012) and Zheleznyakov & Bespalov (2018), we assume that the source is a neutral current sheet filled with an inhomogeneous non-relativistic plasma, on which a transverse (relative to the current sheet), spatially varying magnetic

field is superimposed (Fig. 4b). In addition, we assume that the plasma contains a small fraction of suprathermal electrons, $N_e \ll N$, with a non-equilibrium velocity distribution function that does not affect the dispersion properties of the medium and ensures efficient generation of plasma waves under DPR conditions. An example of such a function is a velocity distribution of the form

$$N_e = A(y, z, t)\, v_\perp^2 \exp\left(-\frac{v_\parallel^2 + v_\perp^2}{2v_e^2}\right), \tag{6}$$

which was used in the kinetic theory of the DPR effect [see paper Zheleznyakov & Zlotnik (1975a) and review Zheleznyakov et al. (2016)]. Here, $v_\parallel$ and $v_\perp$ are the longitudinal and transverse components of the velocity of suprathermal electrons with respect to the magnetic field **B**, respectively, v_e is the characteristic velocity of suprathermal electrons, and $A(y, z, t)$ is the normalization factor dependent on coordinates and time. For efficient wave generation, the velocity v_e of suprathermal electrons should significantly exceed the thermal velocity of the equilibrium plasma component in the source. The normalization factor $A(y, z, t)$ is determined by the complex processes of the possible transfer of electrons into a magnetic trap from the magnetosphere surrounding the source, the processes of losing (or taking) the energy by particles in the source itself, quasi-linear relaxation processes during the plasma wave excitation, etc. These processes remain uncertain, although, of course, they should sometime become part of a complete theory of the origin of the discussed pulsar bursts in the Crab nebula.

As a specific model of the neutral current sheet, we take the so-called Harris layer (Harris 1962) with a transverse magnetic field superimposed on the layer. In such a layer, the distribution of the magnetic field B and electron density N is described by the following formulas (see Fig. 4b):

$$B_y(z) = -B_m \tanh\left(\frac{z}{\Delta}\right); \quad B_z = B_0(y); \tag{7}$$

$$N(y, z) = N_0(y) \cosh^{-2}\left(\frac{z}{\Delta}\right), \tag{8}$$

where Δ is the thickness of the layer, B_m is the magnetic field in the magnetosphere outside the current sheet, and $B_0(y)$ and $N_0(y)$ are the magnetic field and plasma density, respectively, in the central plane of the current sheet. The field in the central plane is much less than the magnetic field B_m at the periphery of the current sheet,

$$\frac{B_m}{B_0} \equiv \sigma \gg 1. \tag{9}$$

Field lines for the superposition of these magnetic fields and the coordinate system we used are presented in Fig. 4(b).

Version 1. Consider first the simplest case of plasma waves excited at the DPR frequency, where energetic electrons are constantly localized and generate plasma waves only in a narrow layer Δz_e near the plane $z = 0$. In this layer, it is possible to neglect the dependence of N and B_y (i.e. f_L and f_B) on z since in the current sheet the scale Δz_e is much less than the characteristic scales of variation of the cyclotron frequency $L_B \equiv f_B(\partial f_B/\partial z)^{-1} \approx \Delta/\sigma$ and the Langmuir frequency $L_N \equiv f_L(\partial f_L/\partial z)^{-1} \approx \Delta$ along the z-axis. Assuming that the Langmuir and cyclotron frequencies along the y-axis are determined by the formulas

$$f_L(y, z = 0) = f_{L,0}\left(1 + \frac{y}{\Delta_N}\right);$$
$$f_B(y, z = 0) = f_{B,0} = \text{const}, \tag{10}$$

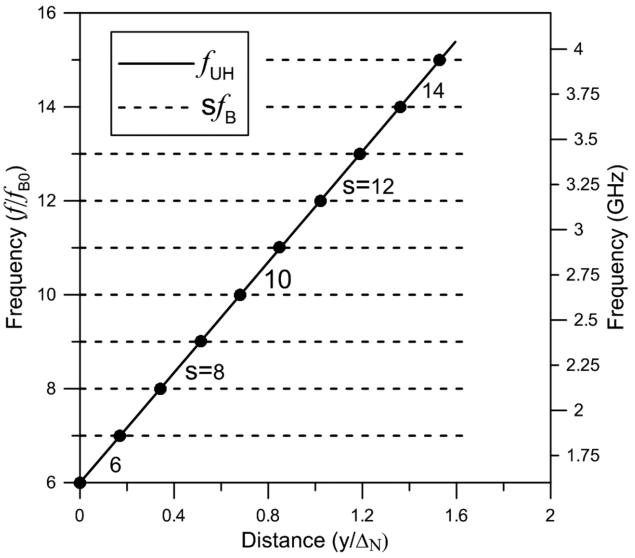

Figure 5. Locations of the DPR points (filled circles), dependence of the electron cyclotron harmonic frequencies sf_B (dashed lines) and the upper-hybrid resonance frequency f_{UH} (solid line) on the distance along the current sheet in the plane $z = 0$ from the point $y = 0$, $z = 0$ (the reference frame is shown in Fig. 4b); Δ_N is a characteristic scale of the plasma density variation; the emission frequency in the source is shown on the right axis. Case $f_B = const$.

and the quantities $f_{L,0}$ and $f_{B,0}$, as follows from (2), are connected by the relationship

$$f_{L,0} = \sqrt{(s_0^2 - 1)}\, f_{B,0}; \tag{11}$$

for one of the harmonics s_0, we obtain the dependence $f_{UH}(y)$

$$f_{UH}(y) = f_{B,0}\sqrt{1 + (s_0^2 - 1)\left(1 + \frac{y}{\Delta_N}\right)^2}. \tag{12}$$

In (10) and (12), $\Delta_N \equiv f_L(\partial f_L/\partial y)^{-1}$ is the characteristic scale of variation of the Langmuir frequency along the y-axis. The value of s_0 was chosen so as to ensure the observed number of emission bands in the dynamic spectrum (Fig. 3) and that the magnetic field in the layer centre does not contradict the values indicated in Zheleznyakov & Bespalov (2018). The dependences of $f_{UH}(y)$ and $sf_B(y)$ on the y-coordinate are given in Fig. 5. The scale on the right indicates the radio emission frequencies in the source provided that plasma waves transform into electromagnetic ones with the frequency preserved, $f_{em} = f$. It was taken into account that for a source moving at velocity $\beta \approx 0.8$, the observed radiation frequency f_{obs} differs by three times from the frequency f_{em} in the source system: $f_{obs} \approx 3f_{em}$. The points where line $f_{UH}(y)$ is intersected by cyclotron harmonic frequency lines sf_B, $f_{UH}(y) = sf_B$, indicate the location of the DPR in the plane $z = 0$, i.e. in the central plane of the current sheet. Note that a specific shape of the function $f_{UH}(y)$ [i.e. $f_L(y)$] is not significant. It is only needed to maintain the monotonic nature of this function [decay or rise of $f_{UH}(y)$] in a frequency range that ensures the generation of a plasma wave spectrum having a width of the order of a few gigahertz. With constant excitation of plasma waves at the DPR frequencies in the plane $z = 0$ during the entire burst, a system of emission bands, shown in Fig. 3, with constant band frequency spacing Δf, is formed in the dynamic spectrum.

Version 2. In the new version, we discuss the formation of a more complex (and more common) dynamic spectrum, an example of

which is shown in Fig. 1. This spectrum is a system of emission bands, each of which consists of a set of bright elements of a fine structure. We associate this version with the generation of plasma waves at the DPR frequency, first in the current sheet near the central plane and then with the propagation (displacement) of this process along the z-axis, i.e. to the DPR frequencies located in the region of the current sheet itself.

Let us first consider how the radiation is generated near the central plane of the current sheet $z = 0$ in this case. As was noted in Section 1, band frequency spacing Δf in the dynamic spectra such as that shown in Fig. 1 varies in proportion to the emission frequency f according to the law (1). It follows that if the appearance of quasi-harmonic emission bands is due to the generation of radiation at the DPR points $f_{\rm UH} = sf_{\rm B}$, then the band frequency spacing should vary with the emission frequency $f \approx sf_{\rm B} = f_{\rm UH}$ according to the law (1), i.e. the cyclotron frequency, unlike version 1, should vary along the y-axis.

Let the cyclotron frequency in the central plane of the current sheet vary linearly along y

$$f_{\rm B}(y) = f_{\rm B,0}\left(1 + \frac{y}{\Delta_{\rm B}}\right); \quad \Delta_{\rm B} = {\rm const}, \tag{13}$$

and the Langmuir frequency is described (10). The quantities $f_{\rm B,\,0}$ and $f_{\rm L,\,0}$ in (10) and (13) are related, as previously, by equality (11). In this case, the upper-hybrid resonance frequency is determined by the formula

$$f_{\rm UH}(y) = f_{\rm B,0}\sqrt{\left(1 + \frac{y}{\Delta_{\rm B}}\right)^2 + (s_0^2 - 1)\left(1 + \frac{y}{\Delta_{\rm N}}\right)^2}. \tag{14}$$

In plasma with cyclotron $f_{\rm B}(y)$ and Langmuir $f_{\rm L}(y)$ frequencies increasing along the y-axis, the frequency spacing of the DPR points in the approximation $f_{\rm L} \gg f_{\rm B}$ is equal to[2]

$$\Delta f = \frac{f\,\Delta_{{\rm B},s}}{s\Delta_{{\rm N},s} - (s+1)\Delta_{{\rm B},s}}, \tag{15}$$

where $\Delta_{{\rm B},s} \equiv f_{\rm B}\,(\partial f_{\rm B}/\partial y)^{-1}_{y=y_s}$ and $\Delta_{{\rm N},s} \equiv f_{\rm L}\,(\partial f_{\rm L}/\partial y)^{-1}_{y=y_s}$ are characteristic variation scales of the cyclotron and Langmuir frequencies, respectively, along the current sheet near the DPR point at the harmonic s.

In view of (1) and the fact that $\Delta_{{\rm B},\,s} = \Delta_{\rm B} = const$, relationship (15) can be rewritten as follows:

$$\Delta_{{\rm N},s} = \frac{1 + 0.06(s+1)}{0.06\,s}\,\Delta_{\rm B}. \tag{16}$$

This expression determines the dependence of $\Delta_{{\rm N},\,s}$ on the scale $\Delta_{\rm B}$ and the number of the harmonic s.

The dependences of the upper-hybrid resonance frequency (14) and harmonics of the cyclotron frequency (13) on the y coordinate are shown in Fig. 6. The points of intersection of the lines of the upper-hybrid resonance frequency $f_{\rm UH}(y)$ and frequencies of the harmonics $sf_{\rm B}$ indicate the location of the DPR in the plane $z = 0$. When plotting the diagrams, it was taken into account that the characteristic scales $\Delta_{\rm B}$ and $\Delta_{\rm N}$ in (13) and (14) in the vicinity of point of DPR with harmonic s are connected by relationship (16). The value of s_0 (as in version 1) was chosen so as to ensure the

[2]The relationship (15) differs from a similar relationship obtained in Zheleznyakov & Zlotnik (1975c). This is due to the difference in the variation of the magnetic field and plasma density in our paper and in Zheleznyakov & Zlotnik (1975c). In Zheleznyakov & Zlotnik (1975c), the higher DPR frequency is due to the higher cyclotron harmonic, while in our paper the higher DPR frequency is due to the lower cyclotron harmonic.

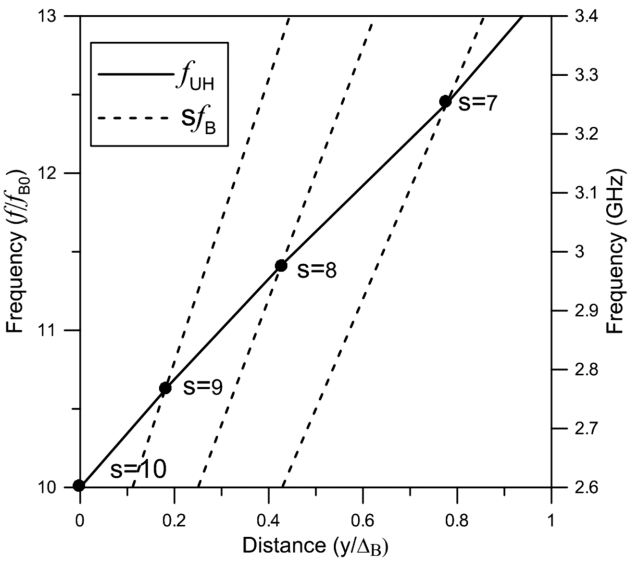

Figure 6. Locations of the DPR points (filled circles), dependence of the electron cyclotron harmonic frequencies $sf_{\rm B}$ (dashed lines) and the upper-hybrid resonance frequency $f_{\rm UH}$ (solid line) on the distance along the current sheet in the plane $z = 0$ from the point $y = 0$, $z = 0$ (the reference frame is shown in Fig. 4b); $\Delta_{\rm B}$ is a characteristic scale of the magnetic field variation; the emission frequency in the source is shown on the right axis. Case $f_{\rm B} \neq const$.

observed number of emission bands (in the considered example, they are four) in the dynamic spectrum in Fig. 1, while the magnetic field in the layer centre did not contradict the value $B = B_z \sim 10^2$ G, shown in Zheleznyakov & Bespalov (2018). The scale on the right indicates the radio emission frequencies provided that plasma waves transform into electromagnetic waves with the frequency preserved. As a result, a system of frequency bands of the type shown in Fig. 1 with the emission band frequency spacing Δf determined by relationship (1) will be observed in the dynamic spectrum.

We now consider what occurs when the fraction of emitting energetic electrons shifts from the central plane along the z-axis into the region $|z| \neq 0$. In this case, the suprathermal electrons generating plasma waves at the harmonic s in the layer centre at the DPR point with the coordinates $y = y_s$, $z = 0$ will successively reach the DPR points lying in the region $z > 0$.

We focus on the process of formation of the fine structure of emission bands due to the DPR effect when the fraction of suprathermal electrons shifts away from the central plane. For this, it suffices to consider the formation of one emission band (fragment of the dynamic spectrum enclosed in a rectangle in Fig. 2), and the structure of the remaining bands can be obtained by analogy. Indeed, in the current sheet, the characteristic scales of the plasma parameters $\Delta_{\rm B}$ and $\Delta_{\rm N}$ along the layer (along the y-axis) are much greater than the characteristic variation scales of the plasma parameters $L_{\rm B}$ and $L_{\rm N}$ across the layer (along the z-axis). In this approximation, it can be assumed that the DPR points with harmonic s at $|z| \neq 0$ are located in the plane $y = y_s$, and their location on the z-axis depends only on the magnetic field and plasma density variations along this axis.

Assume that the magnetic field and plasma density in the current sheet with superimposed transverse magnetic field are described by equations (7), (8), (10), and (13), in which the parameter σ is determined in (9) and the scales of $\Delta_{\rm B}$ and $\Delta_{\rm N}$ are connected by relationship (12). For definiteness, we assume that $s = s_0 = 10$ (see

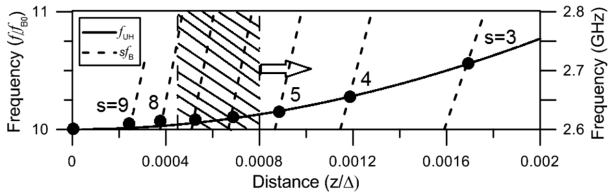

Figure 7. Locations of the DPR points (filled circles) within one frequency interval (sf_{B0}, $(s+1)f_{Bo}$), dependence of the electron cyclotron harmonic frequencies sf_B (dashed lines) and the upper-hybrid resonance frequency f_{UH} (solid line) on the distance across the current sheet in the plane $y = 0$ from the point $y = 0$, $z = 0$ (the reference frame is shown in Fig. 4); Δ is the size of the current sheet. The arrow shows the direction of motion of the suprathermal electrons; the emission frequency in the source is shown on the right axis.

Fig. 6) and $\sigma = 2000$ and place the origin of coordinates to the point $y = y_{s0} = 0$, $z = 0$. In this case, the cyclotron frequency and the upper-hybrid resonance frequency in the plane $y = y_s = 0$ along the z-axis change as follows:

$$f_B(y_s z) = f_{B,0}\sqrt{1+\sigma^2\tanh^2\left(\frac{z}{\Delta}\right)}; \quad (17)$$

$$f_{UH}(y_s, z) = f_{B,0}\left(1+\sigma^2\tanh^2\left(\frac{z}{\Delta}\right) + (s_0^2-1)\cosh^{-2}\left(\frac{z}{\Delta}\right)\right)^{1/2}. \quad (18)$$

Fig. 7 shows the dependence of the z coordinate of the upper-hybrid resonance f_{UH} and cyclotron frequency harmonics sf_B in the plane $y = y_s = 0$ passing through the DPR point with the harmonic $s = 10$ at the centre of the current sheet. The points of intersection of the lines of the upper-hybrid resonance $f_{UH}(z)$ and frequencies of the harmonics $sf_B(z)$ indicate the location of the DPR in the plane $y = 0$. As in Figs 5 and 6, the scale on the right indicates the emission frequencies in the source provided that plasma waves transform into electromagnetic ones with the frequency preserved. The shaded areas with an arrow is a schematic representation of the fraction of energetic electrons with a non-equilibrium distribution function (for example, in the form of 6) and their propagation direction in the current sheet. The coordinates of DPR points in Fig. 7 were calculated under the assumption that $\sigma = 2000$. In this case, frequency spacing of the DPR points is in agreement [allowing for the Doppler frequency shift (5)] with the corresponding frequency intervals for the elements of the fine structure of emission quasi-harmonic bands that are seen in the dynamic spectrum in Fig. 1.

The formation of an emission band with a system of bright elements of a fine structure, such as that presented in Fig. 1 and shown schematically in Fig. 2, proceeds as follows. At the initial time, suprathermal electrons are concentrated near the central plane $z = 0$ and the plasma waves are generated due to the cyclotron instability at the DPR point located in this plane. However, suprathermal electrons then propagate to the region $|z| \neq 0$. As soon as the leading edge of the band containing the fraction of energetic electrons (excitation band) reaches the next DPR point, the plasma waves start to be generated at a frequency corresponding to this resonance. As follows from Fig. 7, this frequency is higher than the previous one. The transformation of excited plasma waves into electromagnetic radiation leads to the appearance of a fine structure. Each element of the structure ends when the trailing edge of the excitation band leaves this DPR point. Thus, the number of simultaneously excited elements is determined by the length of the band of suprathermal electrons along the z-axis. The repetition of this process at several DPR points creates in aggregate a system of thin bright elements in the dynamic spectrum as part of a single emission band, as can be seen in Fig. 2. Since, according to Fig. 7, each subsequent DPR frequency is higher than the previous one, the frequency shift of the fine structure in the dynamic radiation spectrum will look like an upward drift in the frequency of the emission band formed by these elements. Note that this result is in good agreement with the observations by Hankins et al. (2016), who pointed out that the appearance of an upward drift of emission bands is due to the appearance of new elements whose generation is delayed in time and occurs at higher frequencies.

4 CONCLUSION

First of all, we comment on the geometry of the local source considered in the paper. To explain the origin of the quasi-harmonic bands with a fine structure, we considered a planar configuration where the magnetic field and plasma density in the current sheet depend only on two coordinates, y and z, and are independent of the third coordinate x (Fig. 4b). This statement is valid in the case where the sizes of the layer in the third dimension significantly exceed the sizes of the layer in the y, z plane. We also limited ourselves to the natural case where the scale of variation in plasma parameters along the current sheet exceeds the characteristic scale of variation in the magnetic field across the layer. This made it possible to clearly identify the factors determining the formation of the basic properties of the fine structure of emission bands in the dynamic radiation spectra.

Thus, in this work, based on the DPR effect at electron cyclotron harmonics, a detailed and consistent explanation is given for the origin of the quasi-harmonic emission bands with the fine frequency and temporal structure observed in HFIP. According to the proposed scheme, radiation is generated in a local formation – a neutral current sheet with a transverse magnetic field, in areas where the DPR condition $f_L \approx sf_B$ is fulfilled. The structure of the radiation spectrum is determined by the nature of the inhomogeneity of the plasma and magnetic field in the current sheet. The position of the emission bands in the dynamic spectrum and their frequency spacing depend on variations in the plasma and magnetic field along the current sheet; their fine structure is determined by variations in the corresponding parameters in the direction orthogonal to the sheet and the time evolution of suprathermal emitting electrons. In other words, only the DPR condition $f_L \approx sf_B$, the inhomogeneous nature of the plasma and magnetic field, and the time evolution of suprathermal emitting electrons in the local source determine the structure of the dynamic radiation spectrum in HFIP. Note that the DPR condition $f_L \approx sf_B$ does not depend on the corpuscular composition of the plasma in the local source, electron–proton or electron–positron. The choice of the electron–proton variant in this paper is due to the fact that the DPR effect in such plasma is well studied, while the case of the electron–positron composition needs special consideration.

It should be noted that for implementation of the proposed emission mechanism in the form of quasi-harmonic emission bands with fine structure, the conditions in the HFIP source that are unusual for the current widely discussed theories of pulsar magnetospheres are necessary. However, the observation of quasi-harmonic emission bands and, moreover, the fine frequency structure of these bands and the possibility of a detailed and consistent explanation of their origin based on the DPR effect indicate the possibility of the existence of local source with such parameters.

In this paper, one problem, namely the origin of the fine structure of emission bands and their time evolution, was considered in detail. A number of problems associated with the HFIP theory (the origin of the non-relativistic plasma, the current sheet, the formation of a non-equilibrium distribution function of suprathermal electrons, and the drift of these particles across the current sheet) remained outside the scope of this work. Solving all of these problems is an important task that opens up a possibility for diagnosing a local HFIP source in Crab pulsar.

ACKNOWLEDGEMENTS

The work was supported by the Russian Foundation for Basic Research (projects 19-02-00704a and 20-02-00104a) and by the State Assignment No. 0035-2019-0002. The work of V. E. Shaposhnikov (numerical calculations) is supported by the Russian Science Foundation under grant No. 20-12-00268.

REFERENCES

Eilek J. A., Hankins T. H., 2006, in Becker W., Huang H. H., eds, Proc. 363. WE-Heraeus, Neutron Stars and Pulsars, MPE Report 291. Max Planck Institut für extraterrestrische Physik, Garching bei München, Germany, p. 112

Eilek J. A., Hankins T. H., 2016, J. Plasma Phys., 82, 635820302

Hankins T. H., Eilek J. A., 2007, ApJ, 670, 693

Hankins T. H., Rankin J. M., Eilek J. A., 2009, What is the physics of pulsar radio emission? Available at: https://science.nrao.edu/science/astro2010/rac/Hankins_pulsar_physics_SSE.pdf

Hankins T. H., Eilek J. A., Jones G., 2016, ApJ, 833, 47

Harris E. G., 1962, Nuovo Cimento, 23, 115

Kuijpers J., 1975, A&A, 40, 405

Smith F. G., 1969, Nature, 223, 234

Zheleznyakov V. V., 1971, Ap&SS, 13, 87

Zheleznyakov V. V., 1996, Radiation in Astrophysical Plasmas, Astrophysics & Space Science Library, Vol. 204. Kluwer Acad. Publ., Dordrecht, Dordrecht

Zheleznyakov V. V., Bespalov P. A., 2018, Astron. Lett., 44, 442

Zheleznyakov V. V., Zlotnik E. Y., 1975a, Sol. Phys., 43, 431

Zheleznyakov V. V., Zlotnik E. Y., 1975b, Sol. Phys., 44, 447

Zheleznyakov V. V., Zlotnik E. Y., 1975c, Sol. Phys., 44, 461

Zheleznyakov V. V., Zlotnik E. Y., Zaitsev V. V., 2012, Astron. Lett., 38, 589

Zheleznyakov V. V., Zlotnik E. Y., Zaitsev V. V., Shaposhnikov V. E., 2016, Phys. Usp., 59, 997

This paper has been typeset from a TEX/LATEX file prepared by the author.